MONOTONIC VECTOR FORCES AND GREEN'S THEOREM FOR AUTOMATIC AREA CALCULATION

Nikolay Metodiev Sirakov

Department of Mathematics, Department of Computer Science
Texas A&M University-Commerce
Commerce, TX 75429
Ph: 903 886 5943, Fax: 903 886 5945
Email: Nikolay_Sirakov@tamu-commerce.edu

ABSTRACT

The disorders caused by a cerebral hemorrhage depend on its location, shape and area. The purpose of this paper is to develop a framework to automatically extract the above features for the goal of indexing and fast image retrieval. The method uses monotonic normal and tangent forces, defined on an active contour, guided by two forms of the geometric heat equation toward objects' and voids' boundaries, which are used by the Green's Theorem to automatically calculate their areas. To validate the theory experiments are performed with medical images. A discussion on the advantages/limitations and a comparison with existing methods is given at the end of the paper.

Keywords: Active Contour, Geometric Features, Extraction

1. INTRODUCTION

The problems of image indexing and image database (IDB) management affect the correct and quick retrieval of a narrow set of images from large and dynamic IDB. Various features are extracted for this purpose [3,5,8]: low level such as texture, edges, corners [9]; high level such as locations, identified objects, relations between them, and events [2].

Also, many practical problems in medicine depend on the area [11], perimeter and location of certain objects, as well as their rate of change over time. For example, cerebral hemorrhage can cause disorders, because it suppresses brain centers responsible for different human body's activities [1]. Moreover, the intracerebral brain hemorrhage (ICH), its shape and structure is related to the mortality and morbidity [10]. Thus, features subject of interest are: area (volume), position in the image (in space), shape and correlation between regions. The preliminary studies indicate that the ICH area (volume) is significant for the right treatment and survival of the patient [10].

In [12,13,14] new approaches and tools are introduced capable of quick, automatic image segmentation to multiple objects and extraction of the following geometric features: convex hull, number of boundary concavities, their shape, area and perimeter.

Based on the above methods, the present paper develops a framework capable of automatically calculating the area of image regions and voids. The framework could also be used to measure the rate of change of the features, and to determine image semantics in terms of regions' relations. To automatically extract the area a monotonic force is defined on an active contour, guided by two forms of the geometric heat equation [12,13,14]. A stability convergence condition developed in [14] guarantees that the active contour converges without self intersections and curls. The latter allows for application of Green's Theorem to develop a time efficient equation to compute the areas. The calculation complexity of this equation is $O(n)$, where n represents the force's dimension. To validate the theory a set of experiments is performed using medical images.

2. THE MAIN FRAMEWORK'S COMPONENTS

The basic approaches of the automatic area calculation framework are presented in [12,13,14]. This section summarizes the framework and introduces a new algorithm:

1) *Shell algorithm* employs centripetal normal force to segment an image to multiple regions called shells. Each region contains a single object, with respect to its visibility from the force, and automatically defines an initial curve inscribing the object [12,14];

2) The active convex hull model (*ACHM*) is developed in [14] to determine the convex hull (C^H) (Fig.1 (e), (f)) of an object. *ACHM* uses the difference between normal and tangent forces (Fig.1 (a),(c),(f)) determined on each initial curve evolved by the following form of the geometric heat equation: $\frac{\partial C}{\partial t} = P\frac{d\vec{\tau}}{ds} - |dr|\vec{T}$. (1)

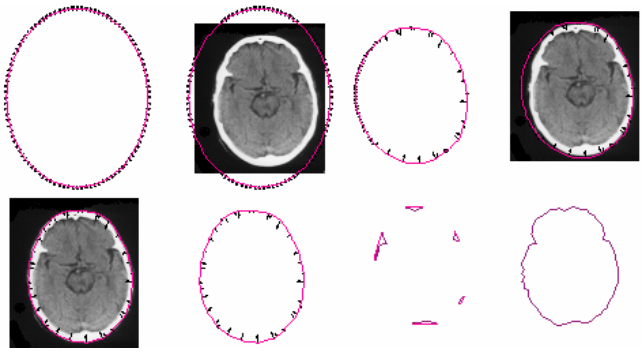

a) b) c) d)
e) f) g) h)

Figure1. a) The active C^H and its force after 100 iterations; **b)** together with a brain section; **c)** and **d)** the same components after 500 iterations; **e)** the C^H, the remaining force and the object; **f)** the C^H and the remaining force; **g)** the concavities of the internal boundary; **h)** the extracted internal boundary of the object.

In Eq.1 C is a smooth, convex, closed curve parameterized by $C(t,s)=r(t,s)=x(t,s)i+y(t,s)j$ in the domain [-1,1]x[-1,1], where $t\in[0,\infty)$ is a time parameter, whereas s is a space parameter, which parameterizes the particular curve; $\vec{T}$ is the tangent vector, whereas $\vec{\tau}=\frac{x_s 2}{nc}i+\frac{y_s 2}{nr}j$ is the tangent vector normalized by the image's sizes - number of columns and number of rows [14]; P denotes a penalty function designed to calculate the rate of change of the image function on the interval $\Delta_t \in \vec{N}=\frac{1}{k}\frac{d\vec{\tau}}{ds}$, where k is the curvature, and $\vec{N}$ is a normal force. P halts evolution for those vectors for which $\varepsilon_1 \geq P(\Delta_t) \geq \varepsilon$. The numbers $\varepsilon_1, \varepsilon$ are given by the user and show the difference between background and foreground, whereas Δ_t gives the number of foreground pixels a vector should encounter in order to stop evolvement [12,14].

An important property of the normal force is that the flow preserves and increases the length of the normal vectors at C^H vertices, whereas the vectors on C^H's straight segments vanish, because the derivative is zero there (Fig.1 (c),(f)). During the time of convergence the tangent force does not change its dimension but decreases the size of the vectors.

3) The active contour model (*ACM*), performs re-parameterization of the C^H to increase the dimension of the normal force and evolves the C^H to the boundary of the object (Figs.1, 2):

$$\frac{\partial C}{\partial t}=P\frac{d\vec{\tau}}{ds}. \qquad (2)$$

4) The new approach, added to the framework by this paper, uses the C^H as an initial contour, re-parameterizes it and switches the meaning of the image's foreground and background. Then, applies shell algorithm and Eq.2, which evolves every contour toward its mass center. Thus, voids' and concavities' boundaries are determined (Figs. 3 and 4). A boundary "closed" by a single C^H edge (Figs. 1(g), 3(d),4(d)) [12] is considered concavity's boundary, otherwise it is a void's boundary.

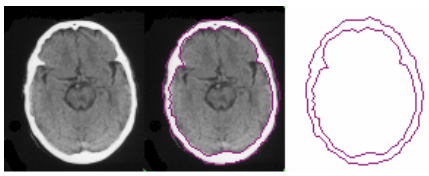

a) b) c)

Figure2. a) The inter-cerebral brain section from Fig.1; **b)** the section and its contours; **c)** the contours alone.

Figs.3 and 4 illustrate the results obtained after applying the framework described above. The objects', concavities' and voids' boundaries are shown in Figs. 3 and 4 (c), (d).

3. OBJECT'S AREA CALCULATION

The problem of image regions' area calculation is not new and has many solutions published in the literature. For example Adobe Photoshop calculates it by using histograms. Mathematical morphology applies operations such as erosion and dilation [7] for this purpose.

The present section develops a new approach for automatic objects' and voids' area calculation applying Green's Theorem and monotonic vector forces defined on active contours, guided by the geometric heat equation in the forms of Eqs.1, 2.

Consider an image containing multiple objects. The application of the *shell algorithm* inscribes every object in a closed, smooth convex curve, whose center lies in the interior of the object. Next, employ ACHM to evolve the contour $C(x(t,s),y(t,s))$ to the C^H, which is constructed as a closed polygon, on which the normal vectors remain at joint points between the C^H and the real boundary. Since $C(t,s)$ converges to C^H without curls and self-intersections the Green's Theorem states that the area of the C^H is:

$$A_{C^H}=\frac{1}{2}\oint_{C^H} xdy-ydx\,, \qquad (3)$$

where x and y are the parametric functions in the definition of the curve C. Using finite differences to approximate derivatives we receive the following discrete presentation of Eq.3:

$$A_{C^H}\approx\frac{1}{2}\sum_{i=1}^{p}(x_i y_{i+1}-x_{i+1}y_i)\,. \qquad (4)$$

In Eq.4 we consider $(p+1)_{MODp}=1$, which means that the $(p+1)^{st}$ vector is actually the first one, and p denotes the number of vectors normal to the C^H. As one can tell the calculation complexity of Eq.4 is on the order of $O(p)$, where $p<n$ - which is the dimension of the force on the initial contour.

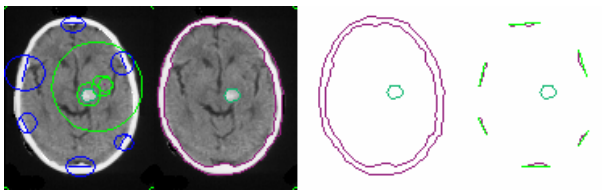

a) b) c) d)

Figure3. a) 2nd section of the same brain with a presence of hemorrhage; **b)** the section and its boundaries; **c)** the brain's and hemorrhage's boundaries; **d)** the void and concavities.

As explained at the end of section 2 the C^H is now re-parameterized in order to increase the normal force dimension, and the meaning of the foreground and the background is switched. Thus concavities and voids are considered "objects" whereas the object's interior as a background. Then the *shell algorithm* inscribes every void and concavity in a circle (Figs. 3 (a), 4 (a)) considered by the *ACM* as initial contours. Then the *ACM* guides each contour to the boundary of the corresponding void and concavity. Therefore the object's area A_O is given by:

$$A_O = A_{C^H} - A_{VCO}\ , \qquad (5)$$

where A_{C^H} denotes the area of the convex hull, whereas A_{VCO} shows the area of all voids and concavities. Obviously the area of a convex object is $A_O = A_{C^H}$, because no voids and concavities are present.

Assume q voids and concavities are present and their boundaries are determined as closed polygon. Recall that the shell algorithm uses the normal force, which is ordered counterclockwise. Therefore an order is introduced among the concavities' and voids' whose area is calculated by the Green's Theorem and Eq.3:

$$A_{VCO} = \frac{1}{2}\sum_{u=1}^{q}\oint_{C_U} x_u dy_u - y_u dx_u\ . \qquad (6)$$

In Eq.6 x_u, y_u are the parametric functions in the definition of the u^{th} active contour determined by the *shell algorithm*. Using finite differences we receive the following discrete form of Eq.6:

$$A_{VCO} \approx \frac{1}{2}\sum_{u=1}^{q}\sum_{i=1}^{p_u}(x_{ui}y_{u(i+1)} - x_{u(i+1)}y_{ui})\ . \qquad (7)$$

In Eq.7 p_u represents the number of normal vectors on the *u-th* boundary determined by the *u-th* active contour, and $p_i \neq p_j$ if $i \neq j$. Also, $(x_{ui}, _{ui})$ in Eq.7 are obtained by adding the mass-center, of the object in the *u-th* shell, to the coordinates of the boundary vertices determined by the corresponding active contour. It holds because the latter coordinates are calculated with respect to the mass-center (center of the active contour), whereas the coordinates in Eq.7 are with respect to the origin of the image.

Note that the above algorithm does not distinguish between voids and concavities. Recall that a boundary

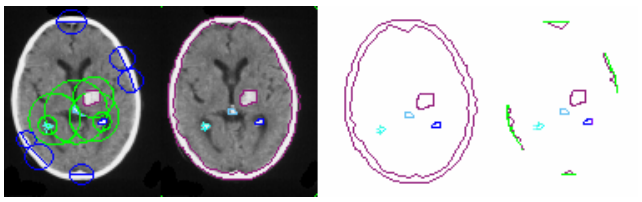

a) b) c) d)

Figure4. a) 3rd inter-cerebral section with 4 hemorrhages; **b)** the section, the brain's and hemorrhages' boundaries; **c)** the boundaries alone; **d)** the hemorrhages and concavities.

"closed" by a single C^H edge [12] is considered concavity, otherwise it is a void. Using this concept the set of voids is easily separated from the set of boundary concavities. Follows, the area of the voids A_V and the area of the concavities A_{CO} could be calculated separately using Eqs.6 and 7 for each set, if it is needed for indexing, or recognition and retrieval purposes

4. EXPERIMENTAL RESULTS

To validate the theoretical concepts experiments were performed using inter-cerebral sections with hemorrhage shown in Figs.3 and 4. A C++ implementation was run for this purpose on a PC with a clock frequency 1.8 GHz. The image in Fig.3 (a) is of size 96x114. Employing the area calculation algorithm the convex hull of the brain as well as the brain's concavities and hemorrhages were extracted (Fig.3 (c),(d)). Employing Eq.4 the C^H area was determined to be $A_{C^H} = 5352$ pixels. Applying Eqs.6, and 7 it was calculated that $A_{VCO} = 164$, which yields $A_O = A_{C^H} - A_{VCO} = 5188$. The area measured using Adobe Photoshop functions "magic wands" and "histograms" the area of the brain section was calculated to be 5153, which yields an error of 35 pixels. The latter number gives an error of 0.7% with respect to the object's area.

It follows from the theory that the error of boundary approximation is less than $n\Delta_t$, where n denotes the number of vectors normal to the initial active contour, and Δ_t shows the number of pixels a normal vector should penetrate an image region in order to stop evolvement.

The same procedure, as explained above, was used to determine the brain area and the area of the hemorrhages given in Fig.4 (a). The image is of size 96x114. Thus the area of the convex hull of the brain is $A_{C^H} = 5371$. The total area of the hemorrhages and concavities calculated by Eq.7 is $A_V = 292$, whereas the area of the concavities is $A_{CO} = 146$ pixels, and the area of the hemorrhages alone is $A_V = 146$ pixels. Thus, the total brain area is $A_O = 5088$ pixels. The area measured by using Adobe Photoshop is 5048 pixels, which yields an error of 40 pixels or 0.79%.

The following notations are used in Table1: FD denotes the force dimension, in *n/m* the number *n* denotes the vector force's dimension on the initial contour, m- on the convex hull after re-parameterization; in the column for Δ_t - the first digit shows the number of pixels used to determine the C^H, whereas the second one is used to determine concavities' and voids' boundaries; *run* - denotes the run time, in seconds, for the segmentation approach. EA denotes the error of object's area calculation in percents.

Table 1

Fig	void	FD	Δ_t	run	A_O	A_V	A_{CO}	EA
2	No	90/80	4/6	0.22	4851	0	N/A	N/A
3	1	90/80	6/4	0.32	5188	73	91	0.7
4	4	90/130	4/3	0.4	5088	146	146	0.79

5. CONCLUSSIONS AND FUTURE WORK

A contribution of this work is the application of monotonic normal force guided by two forms of the heat equation toward boundaries used by the Green's Theorem for objects' and voids' area calculation. The active contour models and level set methods are powerful tools to be applied for this purpose [4,6,11,15,16]. The paper [15] develops a method to determine the boundary of a brain tumor, but area calculation is not provided. In [11] an active contour is employed to compute the area of leg ulcers, but the model uses manual delineation process in order to initialize the solution. Recall that the present framework is automatic and the initial contour inscribes the entire image. Another advantage is that the area calculations are on the order of *O(n)***.** Since the framework needs a set of settings (Δ_t, FD, $\varepsilon, \varepsilon_1$), their choice turns out to be a disadvantage.

To distinguish concavities from voids an algorithm is used based on the statement that each concavity's boundary is closed by a single C^H edge [12].

Another effective approach for area calculation is given in [7]. It employs a bi-tangent as a concavity's edge and Morphological erosions and deletions, with calculation complexity *O(N)*, where *N* is the number of the grid points. Considering that in our framework *n* is the force dimension, follows that *n*<*N*, which shows that our methods is more effective, providing fewer arithmetic operations.

Our future research aims to extend the present framework and employ the monotonic forces to determine semantic-objects' relations and events.

6. ACKNOWLEDGEMENT

Part of this research is supported by Research Enhancement project funded by the School of Graduate Studies, TAMUC. Thanks to Dr. Kreminski for the helpful discussions on the Green's Theorem application.

7. REFERENCES

[1] Chia-Ying Lu et al, Detection of intracranial hemorrhage. Comparison between gradient-echo images and b0 images obtained from diffusion-weighted echo-planar sequences on 3.0T MRI, J of Clinical Imaging , V29, Issue 3 , 05-2005, pp 155-161

[2] M. Cord, P. H. Gosselin, "Image Retrieval Using Long-Term Semantic Learning", IEEE ICIP2006, Atlanta, October 2006, pp.2209-2212.

[3] A. Del Bimbo and P. Pala, "Shape Indexing by Multi-Scale Representation", Image and Vision Computing, v. 17, n. 3-4, pp. 245-261, 1999.

[4] R.P. Fedkiw, G. Sapiro, C. Shu**, "**Shock capturing, level sets, and PDE based methods in computer vision and image processing: a review of Osher's contributions," Journal of Computational Physics, Volume 185, Issue 2, 1 March 2003, Pages 309-341

[5] T. Gadi, et al., "Fuzzy Similarity Measure for Shape Retrieval," Proc. of the Conf. Vision Interface '99, Trois-Rivieres, Canada, pp. 386-389, May 1999.

[6] X. Han, C. Xu, and J. L. Prince, "A Topology Preserving Level Set Method for Geometric Deformable Models," IEEE Tran on Pattern Anal and Machine Intell, Vol 25, No 6, pp.755-768, 2003.

[7] J. L. Lisani, et al., "Affine Invariant Mathematical Morphology Applied to a Generic Shape Recognition Algorithm", Math Morph and its Appl to Image and Signal Proc., J. Goutsias, L.Vincent, D.Bloomberg (eds.), Kluwer Acad. Pub, pp. 91-98, 2000.

[8] Liu, Y., Lazar, N., Rothfus, W., et al., Trends and Advances in Content-Based Image and Video Retrieval, Shapiro, Kriegel, and Veltkamp, ed., February, 2004.

[9] Z. Li, A. K. Katsaggelos, and B. Gandhi, "Fast video shot retrieval based on trace geometry matching", IEEE Proc on Vision, Image and Signal Processing, pp. 367-373, vol. 152(3), May 2005.

[10] S. Loncaric, A. P. Dhawan, "3-D Quantification of Intracerebral Brain Hemorrhage", Annual Report, 1996-1997, University of Zagreb, Croatia, U of Texas Arlington, Project#J198.

[11] D. Tim Jones, P. Plassmann, "An active contour model for measuring the area of leg ulcers," IEEE Trans. Med. Imag., vol. 19, n°12, 2000, pp. 1202-1210 .

[12] N.M. Sirakov, I. Simonelli, "A New Automatic Concavities Extraction Model," IEEE, Computer Society, 2006, USA, 178-182. ISBN: 1-4244-0069-4, Library of Congress #: 2005937121.

[13] N.M. Sirakov, Automatic Concavity's Area Calculation Using Active Contours and Increasing Flow, IEEE ICIP2006, Atlanta, October 2006, pp..*225-228*

[14] N.M. Sirakov, A New Active Convex Hull Model For Image Regions, Journal of Math Imaging and Vision, Vol.26, 2006, pp.309-325. http://dx.doi.org/10.1007/s10851-006-9004-6

[15] Kyeong-Jun Munet et al, Active Contour Model Based Object Contour Detection Using Genetic Algorithm with Wavelet Based Image Preprocessing, Int Journal of Control, Automation, and Systems Vol. 2, No. 1, March 2004, pp.100-106.

[16]G. Unal,, et al.**, "**Semi-Automatic Lymph Node Segmentation In Ln-Mri", IEEE International Conf on Image Processing, ICIP2006, Atlanta, October 2006, pp. 77-80.